# Elimination Reactions of (*E*)- and (*Z*)-Benzaldehyde *O*-Benzoyloximes. Transition State Differences for the Syn- and Anti-Eliminations Forming Nitriles

Bong Rae Cho,* Hak Suk Chung, and Nam Soon Cho

*Department of Chemistry, Korea University, Seoul 136-701, Korea*

*Received February 13, 1998*

Elimination reactions of (*E*)- and (*Z*)-benzaldehyde *O*-benzoyloximes **1** and **2** with DBU in MeCN have been investigated kinetically. The reactions are second order and exhibit substantial values of Hammett $\rho$ and $k_H/k_D$ values, and an E2 mechanism is evident. The rate of elimination from **2** is approximately 36000 fold faster than that from **1**. For reactions of **1** with DBU in MeCN, $k_H/k_D = 3.3 \pm 0.2$, Hammett $\rho$ value of $2.19 \pm 0.05$, $\beta_{1g} = -0.49 \pm 0.02$, $\Delta H^{\ddagger} = 10.4 \pm 0.6$ kcal/mol, and $\Delta S^{\ddagger} = -34.3 \pm 2.6$ eu have been determined. The corresponding values for **2** are $k_H/k_D = 7.3 \pm 0.2$, $\rho = 1.21 \pm 0.05$, $\beta_{1g} = -0.40 \pm 0.01$, $\Delta H^{\ddagger} = 6.8 \pm 0.5$ kcal/mol, and $\Delta S^{\ddagger} = -25.8 \pm 1.9$ eu, respectively. The results indicate that the anti-eliminations from **2** proceed via more symmetrical transition states with smaller degrees of proton transfer and $N_\alpha$−OC(O)Ar bond cleavage, less negative charge development at the $\beta$-carbon, and a greater extent of triple bond formation than that for the syn-elimination.

Recently, we reported that elimination reactions of (*E*)- and (*Z*)-benzaldehyde *O*-pivaloyloximes promoted by 1,8-diazabicyclo[5.4.0]undec-7-ene (DBU) in MeCN proceed by an E2 mechanism.[1] The rate of anti-elimination from the (*Z*)-isomer was approximately 20000-fold faster than that of syn-elimination from the (*E*)-isomer. The transition state for the former appeared to be more symmetrical than that of the latter. However, the transition state differences for the syn- and anti-eliminations has not been elucidated in detail due to the lack of the data for the extent of N-leaving group bond cleavage.

In this work, we have studied the reactions of (*E*)- and (*Z*)-benzaldehyde *O*-benzoyloximes with 1,8-diazabicyclo-[5.4.0]undec-7-ene (DBU) in MeCN (Scheme 1). We have determined the $k_H/k_D$, Hammett $\rho$, and Brönsted $\beta$ values for the elimination reactions. The results provide measures of the effects of isotopic substitution, $k_H/k_D$, the effect of the substituent at the $\beta$-phenyl group, $\rho$, and the effects of leaving group basicity, $\beta_{1g}$, on the rate and on each other for both reactions. The structure−reactivity parameters that have been obtained permit a mapping of the transition state for these reactions on the More−O'Ferral−Jencks reaction coordinate energy diagram. These results provide a more complete picture of the transition state differences for the syn- and anti-eliminations forming nitriles.

## Results

(*E*)-Benzaldehyde *O*-benzoyloximes were prepared by the literature method.[3] (*Z*)-Benzaldehyde *O*-benzoyloximes were synthesized in reasonable yields by reacting the (*Z*)-benzaldoximes with benzoyl chloride at −40 °C in pyridine solution. The deuterated compounds **1aa′**−**d′**-$d_1$, **1da′**-$d_1$, **2ab′**−**d′**-$d_1$, and **2da′**-$d_1$ were prepared by using the benzaldehyde-$d_1$ and *p*-nitrobenzaldehyde-$d_1$ by the same procedure.[1,3−5]

The reactions of **1aa′** and **2aa′** with DBU in MeCN produced benzonitrile and benzoate. The GC yields of the benzonitrile from the reactions of **1aa′** and **2aa′** with DBU were 99 and 93%, respectively. No trace of benzaldoxime could be detected either by GC or TLC.

Rates of eliminations from **1** and **2** were followed by monitoring the decrease in the absorption at the $\lambda_{max}$ for the reactants in the range of 260−292 nm with a UV-vis or a stopped-flow spectrophotometer. Excellent pseudo-first-order kinetic plots that covered at least two half-lives were obtained. However, reactions of **1aa′**−**c′**, **1ba′**−**c′**, and their deuterated analogs with DBU were too slow to measure the infinity absorption values accurately. Therefore, a Guggenheim method was employed. The rate constants for DBU-promoted eliminations from **1** and **2** are listed in Tables 1 and 2. The $k_2$ values are constant for 5-fold variation in base concentration.

The primary isotope effect values were calculated from the rate coefficients for eliminations from **1aa′**, **1ab′**, **1ac′**, **1ad′**, **1da′**, **2aa′**, **2ac′**, **2ad′**, **2ad′**, and their deuterated analogues. The values are smaller for **1** than for **2** and change only slightly with the change in the aryl substituent. The $k_H/k_D$ values are listed in Table 3.

The influence of the $\beta$-aryl substituents upon the elimination rates gave excellent correlations with $\sigma$ values (Figures S1 and S2 in the Supporting Information). The $\rho$ values are larger for **1** than for **2** and decrease as the electron-withdrawing ability of the aryl substituent increases. Hammett $\rho$ values are summarized in Table 4.

The $k_2$ values showed excellent correlation with the leaving group p$K_a$ values on the Brönsted plot (Figures S3 and S4). The $|\beta_{1g}|$ values are larger for **1** than for **2**

(1) Cho, B. R.; Cho, N. S.; Lee, S. K. *J. Org. Chem.* **1997**, *62*, 2230−2233.
(2) Jencks, W. P. *Chem. Rev.* **1985**, *85*, 511−527.
(3) Cho, B. R.; Jang, W. J.; Bartsch, R. A. *J. Org. Chem.* **1993**, *58*, 3901−3904.
(4) Macco, A. A. *J. Org. Chem.* **1978**, *43*, 1591−1593.
(5) Corey, E. J.; Suggs, J. W. *Tetrahedron Lett.* **1975**, *31*, 2647−2650.

S0022-3263(98)00264-3 CCC: $15.00 
Published on Web 06/18/1998

**Scheme 1**

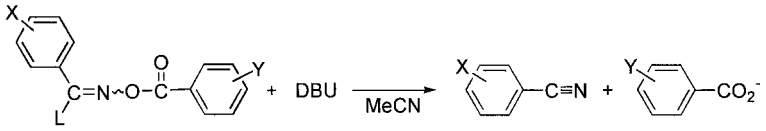


*E*-isomer (**1**), *Z*-isomer (**2**); L = H, D,

X = H (**a**), *p*-MeO (**b**), *m*-Br (**c**), *p*-$NO_2$ (**d**); Y = H (**a'**), *p*-MeO (**b'**), *m*-Br (**c'**), *p*-$NO_2$ (**d'**)

**Table 1. Rate Constants for Eliminations from (*E*)-$XC_6H_4CL{=}NOC(O)C_6H_4Y$[a,b] Promoted by DBU[c,d] in MeCN at 25.0 °C**

| | $10^2k_2$, $M^{-1}$ $s^{-1}$ [e] | | | |
|---|---|---|---|---|
| X and Y | H | *p*-MeO | *m*-Br | *p*-$NO_2$ |
| H | 0.465 ± 0.003[f] | 0.250 ± 0.02 | 2.10 ± 0.14 | 4.38 ± 0.16 |
| H[g] | 0.141 ± 0.008 | 0.0730 ± 0.0013 | 0.600 ± 0.013 | 1.21 ± 0.01 |
| *p*-MeO | 0.122 ± 0.001 | 0.0600 ± 0.005 | 0.700 ± 0.004 | 1.53 ± 0.19 |
| *m*-Br | 2.98 ± 0.05 | 1.31 ± 0.01 | 12.6 ± 0.4 | 23.8 ± 1.2 |
| *p*-$NO_2$ | 24.8 ± 0.4[h] | 13.4 ± 1.2 | 95.7 ± 3.4 | 149 ± 9 |
| *p*-$NO_2$[g] | 8.90 ± 0.11 | | | |

[a] [Substrate] = (2.00−3.00) × $10^{-5}$ M. [b] L = H except otherwise noted. [c] DBU = 1,8-diazabicyclo[5.4.0]undec-7-ene. [d] [DBU] = (2.00−10.0) × $10^{-2}$ M. [e] Average and standard deviation for two or more kinetic runs. [f] $k_2$ = 2.59 × $10^{-3}$ and 9.00 × $10^{-3}$ $M^{-1}$ $s^{-1}$ at 15.0 and 35.0 °C, respectively. [g] L = D.

**Table 2. Rate Constants for Eliminations from (*Z*)-$XC_6H_4CL{=}NOC(O)C_6H_4Y$[a,b] Promoted by DBU[c,d] in MeCN at 25.0 °C**

| | $10^{-2}k_2$, $M^{-1}$ $s^{-1}$ [e] | | | |
|---|---|---|---|---|
| X and Y | H | *p*-MeO | *m*-Br | *p*-$NO_2$ |
| H | 1.69 ± 0.03[f] | | 5.00 ± 0.07 | 10.8 ± 0.5 |
| H[g] | 0.230 ± 0.001 | | 0.750 ± 0.001 | 1.69 ± 0.01 |
| *p*-MeO | 0.690 ± 0.04 | | 2.42 ± 0.06 | 5.20 ± 0.1 |
| *m*-Br | 4.22 ± 0.07 | 1.73 ± 0.02 | 11.4 ± 0.08 | 26.7 ± 1.7 |
| *p*-$NO_2$ | 13.7 ± 0.34[f] | 6.58 ± 0.10 | 38.7 ± 0.3 | |
| *p*-$NO_2$[g] | 1.52 ± 0.02 | | | |

[a] [Substrate] = (1.30−7.50) × $10^{-4}$ M. [b] L = H except otherwise noted. [c] DBU = 1,8-diazabicyclo[5.4.0]undec-7-ene. [d] [DBU] = (4.88−6.00) × $10^{-2}$ M. [e] Average and standard deviation for two or more kinetic runs. [f] $k_2$ = 2.59 × $10^{-3}$ and 9.00 × $10^{-3}$ $M^{-1}$ $s^{-1}$ at 15.0 and 35.0 °C, respectively. [g] L = D.

**Table 3. Primary Isotope Effect Values for Eliminations from (*E*)- and (*Z*)-$XC_6H_4CL{=}NOC(O)C_6H_4Y$[a] Promoted by DBU in MeCN at 25.0 °C**

| | $k_H/k_D$ | |
|---|---|---|
| Y | *E*-isomer | *Z*-isomer |
| *p*-MeO | 3.4 ± 0.3 | |
| H | 3.3 ± 0.2 (2.8 ± 0.1)[b] | 7.3 ± 0.2 (9.0 ± 0.3)[b] |
| *m*-Br | 3.5 ± 0.3 | 6.7 ± 0.1 |
| *p*-$NO_2$ | 3.6 ± 0.1 | 6.4 ± 0.3 |

[a] X = H except otherwise noted. [b] X = *p*-$NO_2$.

**Table 4. Hammett $\rho$ Values for Eliminations from (*E*)- and (*Z*)-$XC_6H_4CL{=}NOC(O)C_6H_4Y$ Promoted by DBU in MeCN at 25.0 °C**

| | $\rho$ | |
|---|---|---|
| Y | *E*-isomer | *Z*-isomer |
| *p*-MeO | 2.20 ± 0.11 | 1.49[a] |
| H | 2.19 ± 0.05 | 1.21 ± 0.05 |
| *m*-Br | 2.04 ± 0.07 | 1.12 ± 0.06 |
| *p*-$NO_2$ | 1.90 ± 0.05 | 1.06 ± 0.04 |

[a] Calculated with the rate data for **2cb′** and **2db′**.

and decrease as the electron-withdrawing ability of the aryl substituent increases. The $\beta_{1g}$ values are listed in Table 5.

Rates of elimination from **1**, **2** promoted by DBU in MeCN were measured at three temperatures spanning 20 °C. Arrehnius plots exhibited excellent linearity (plots not shown). Calculated enthalpies and entropies of activation are summarized in Table 6.

**Table 5. Values of $\beta_{1g}$ for Eliminations from (*E*)- and (*Z*)-$XC_6H_4CL{=}NOC(O)C_6H_4Y$ Promoted by DBU in MeCN at 25.0 °C**

| | $\beta_{1g}$ | |
|---|---|---|
| X | *E*-isomer | *Z*-isomer |
| *p*-MeO | −0.56 ± 0.03 | −0.44 ± 0.01 |
| H | −0.49 ± 0.02 | −0.40 ± 0.01 |
| *m*-Br | −0.49 ± 0.03 | −0.44 ± 0.03 |
| *p*-$NO_2$ | −0.42 ± 0.04 | −0.42 ± 0.04 |

**Table 6. Relative Rate, $k_H/k_D$, Hammett $\rho$, and $\beta_{1g}$ Values for (*E*)- and (*Z*)-$XC_6H_4CL{=}NOC(O)C_6H_4Y$[a] Promoted by DBU in MeCN at 25.0 °C**

| | *E*-isomer | *Z*-isomer |
|---|---|---|
| relative rate | 1 | 36000 |
| $k_H/k_D$ | 3.3 ± 0.2 | 7.3 ± 0.2 |
| $\rho$[b] | 2.19 ± 0.05 | 1.21 ± 0.05 |
| $\beta_{1g}$[c] | −0.49 ± 0.02 | −0.40 ± 0.01 |
| $\Delta H^{\ddagger}$, kcal/mol[a] | 10.4 ± 0.6 | 6.8 ± 0.5 |
| $\Delta S^{\ddagger}$, eu[a] | −34.3 ± 2.6 | −25.8 ± 1.9 |

[a] X = H, Y = H except otherwise noted. [b] Y = H. [c] X = H.

## Discussion

**Mechanism of Eliminations from 1 and 2 Promoted by DBU in MeCN.** Results of product studies and kinetic investigations reveal that the reactions of **1** and **2** with DBU in MeCN proceed by the E2 mechanism. Since the reactions produced only elimination products and exhibited second-order kinetics, all but bimolecular pathways can be ruled out. In addition, an E1cb mechanism is negated by the substantial values of $k_H/k_D$ and $|\beta_{1g}|$.[6−8] A similar mechanism has been proposed for the nitrile-forming eliminations from benzaldoxime derivatives under various conditions.[9−15]

(6) Saunders, W. H., Jr.; Cockerill, A. F. *Mechanism of Elimination Reactions*; Wiley: New York, 1973; (a) chapter 1−4, (b) pp 498−531.
(7) Lowry, T. H.; Richardson, K. S. *Mechanism and Theory in Organic Chemistry*; Harper and Row: New York, 1987; pp 591−616.
(8) Gandler, J. R. In *The Chemistry of Double Bonded Functional Groups*; Patai, S., Ed.; John Wiley & Sons: Chichester, 1989; Vol. 2, Part 1, pp 734−797.
(9) Hegarty, A. F.; Tuohey, P. J. *J. Chem. Soc., Perkin Trans. 2* **1980**, 1313−1317.

**Transition State Differences for the Syn- and Anti-Eliminations Forming Nitriles.** Previous work has shown that anti-elimination reactions of (*E*)-benzaldehyde *O*-pivaloyloximes promoted by DBU in MeCN proceed at approximately 20000-fold faster rate than that of syn-eliminations from the (*E*)-isomers.[1] The much faster rate of anti-elimination was attributed to the steric strain in the (*Z*)-isomer and the favorable overlap between the developing p orbitals at the $\beta$-carbon and α-nitrogen atoms in the transition state. A similar result is observed for elimination reactions of **1** and **2** (Table 6). Thus the anti/syn rate ratio calculated with the $k_2$ values of $4.65 \times 10^{-3}$ and 169 $M^{-1}$ $s^{-1}$ for **1aa′** and **2aa′**, respectively, is approximately 36000. An ab initio calculation with the 6-31G basis set reveals that the bond lengths and bond angles for both isomers are very similar, although the (*Z*)-isomer is slightly distorted from planarity apparently due to the unfavorable steric interactions between the phenyl and the leaving group (Table S1). In addition, the (*Z*)-isomer is less stable than the (*E*)-isomer by 3.734 kcal/mol. Therefore, the same interpretation can be used to explain the large rate ratio.

The structures of the transition states may be assessed by comparing the Hammett $\rho$, $k_H/k_D$, and $\beta_{1g}$ values. The Hammett $\rho$ value indicates the extent of negative charge development at the $\beta$-carbon. The $\rho$ value for the anti-elimination is much smaller than that for the syn-elimination, indicating a smaller extent of negative charge development at the $\beta$-carbon in the transition state. In contrast, the $k_H/k_D$ value is much larger for the former. In view of the prediction that the $k_H/k_D$ increases until it reaches a maximum value and then decreases as the extent of proton transfer increases, the larger $k_H/k_D$ value may be interpreted as either a greater or a smaller extent of proton transfer in the transition state.[16] However, the latter interpretation is more compatible with the smaller $\rho$ value observed for the anti-eliminations.

The extent of $N_\alpha$−OC(O)Ar bond cleavage may be assessed by comparing the $|\beta_{1g}|$ values. The value is smaller for the anti- than for the syn-elimination, indicating a smaller degree of leaving group bond cleavage in the anti transition state. The activation parameters listed in Table 6 are consistent with this interpretation. The enthalpy of activation is smaller for the former probably because the $C_\beta$−H and $N_\alpha$−OC(O)Ar bonds are broken to lesser extents. In addition, the higher reactant energy of **2** should also decrease the $\Delta H^{\ddagger}$ (*vide supra*). Moreover, since the transition state for the anti-elimination is less associated with respect to the base-proton bond, the entropy of activation should be less negative. Therefore, the transition state for the anti-eliminations from **2** appears to be more symmetrical with a smaller degree of proton transfer, less negative charge development at the $\beta$-carbon, and a smaller extent of leaving group bond cleavage than that for the corresponding syn-eliminations from **1**.

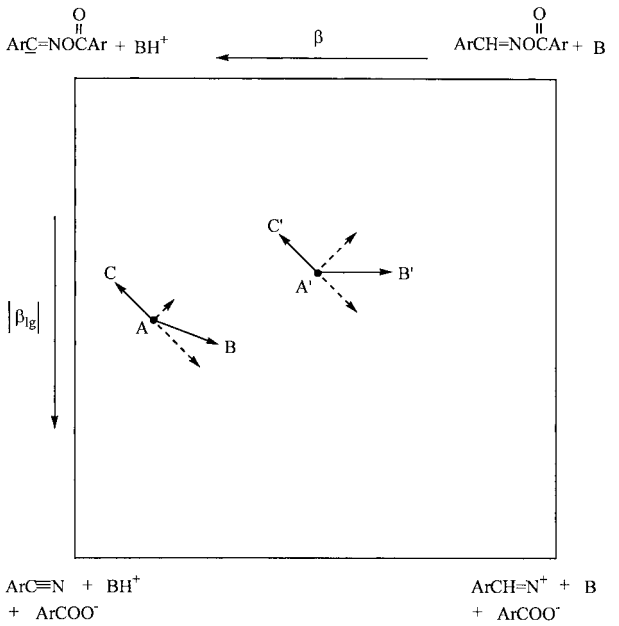


**Figure 1.** Reaction coordinate diagram for nitrile-forming eliminations. The effects of the change to a better leaving group and a stronger electron-withdrawing $\beta$-aryl substituent are shown by the shift of the transition state from A to B and A to C for the *E*-isomer and A′ to B′ and A′ to C′ for the *Z*-isomer, respectively.

**Mapping of the Transition States.** Changes in the structure−reactivity parameters that reflect the changes in the transition state structure provide additional evidences for the above conclusions. These changes can usually be described on the energy surface of More−O'Ferall−Jencks diagram.[2] An energy surface for the elimination reactions of DBU-promoted eliminations from **1** and **2** is shown in Figure 1.

Table 3 shows that the $k_H/k_D$ values for **1** increase slightly as the leaving group is made less basic. Since the smaller isotope effect for the former has been attributed to an extensive proton transfer past halfway (*vide supra*), this result should indicate a gradual decrease in the extent of proton transfer in the transition state. The result can be described by a positive $p_{xy}$ interaction coefficient, $p_{xy} = \partial\beta/\partial pK_{1g} > 0$, which provide additional support for the concerted E2 mechanism.[8,17] On the More−O'Ferall−Jencks energy diagram in Figure 1, a change to a better leaving group will raise the energy of the top edge of the diagram. The transition state with greater extent of proton transfer than $N_\alpha$−OC(O)Ar bond cleavage will then move slightly toward the right as depicted by a shift from A to B on the energy diagram, resulting in a small increase in $k_H/k_D$ (*vide supra*).[2] On the other hand, the $k_H/k_D$ values for **2** decrease with the same variation of the leaving group. The result can also be explained with a decrease in the extent of proton transfer by assuming less than half proton transfer in the former transition state, a positive $p_{xy}$ interaction coefficient, $p_{xy} = \partial\beta/\partial pK_{1g} > 0$, and a shift of the transition state from A′ to B′ in Figure 1.[2,8,17]

The $k_H/k_D$ value decreases for **1** but increases for **2**, respectively, as the electron-withdrawing ability of the

(10) Cho, B. R.; Kim, K. D.; Lee, J. C.; Cho, N. S. *J. Am. Chem. Soc.* **1988**, *110*, 6145−6148.
(11) Cho, B. R.; Lee, J. C.; Cho, N. S.; Kim, K. D. *J. Chem. Soc., Perkin Trans. 2* **1989**, 489−492.
(12) Cho, B. R.; Min, B. K.; Lee, C. W.; Je, J. T. *J. Org. Chem.* **1991**, *56*, 5513−5516.
(13) Cho, B. R.; Jung, J.; Ahn, E. K. *J. Am. Chem. Soc.* **1992**, *114*, 3425−3458.
(14) Cho, B. R.; Je, J. T. *J. Org. Chem.* **1993**, *58*, 6190−6193.
(15) Cho, B. R.; Maing Yoon, C.-O.; Song, K. S. *Tetrahedron Lett.* **1995**, *36*, 3193−3196.
(16) Smith, P. J. In *Isotopes in Organic Chemistry;* Buncel, E., Lee, C. C., Eds.; Elsevier: Amsterdam, 1976; pp 239−241.
(17) Gandler, J. R.; Jencks, W. P. *J. Am. Chem. Soc.* **1982**, *104*, 1937−1951.

b-aryl substituent is increased (Table 3). Since the extent of proton transfer for the two reactions is assumed to be on different sides of the midpoint, these results indicate an increase in the extent of proton transfer in both transition states (*vide supra*). This effect can be described by a positive $p_{xy'}$ interaction coefficient, $p_{xy'} = \partial\beta/\partial\sigma > 0$, and the reaction coordinate that has large components of proton transfer and $N_\alpha$−OC(O)Ar bond cleavage.[8,17] These changes in the $k_H/k_D$ values can be described on the More−O'Ferall−Jencks energy diagram (Figure 1).[2] An electron-withdrawing $\beta$-aryl substituent will lower the energy of the carbanion intermediate in the upper left corner of the diagram. The transition state will then move slightly toward the upper left corner, with more proton transfer and larger or smaller $k_H/k_D$, as depicted by the shifts from A to C and A′ to C′ for **1** and **2**, respectively, on the energy diagram.

As shown in Table 4, there is a progressive decrease in the Hammett $\rho$ values with a better leaving group. This result can be described by a negative $p_{yy'}$ interaction coefficient, $p_{yy'} = -\partial\rho/\partial pK_{1g} = -\partial\beta_{1g}/\partial\sigma < 0$.[8,17] The decrease in the $|\beta_{1g}|$ values with a stronger electron-withdrawing $\beta$-aryl substituent (Table 5) provides additional evidence for this effect, i.e., $p_{yy'} = -\partial\beta_{1g}/\partial\sigma < 0$. The negative $p_{yy'}$ coefficients observed in these reactions are consistent with an E2 mechanism and the reaction coordinates that have large components of proton transfer and $N_\alpha$−OC(O)Ar bond cleavage so that a better leaving group would shift the transition state from A to B and A′ to B′ for **1** and **2**, respectively, to decrease the extent of negative charge development and the $\rho$ values (Figure 1). Moreover, an electron-withdrawing substituent would shift the transition state from A to C for **1** in the direction of decreased $N_\alpha$−OC(O)Ar bond cleavage and smaller $|\beta_{1g}|$ values.[2] The nearly identical $|\beta_{1g}|$ values for **2** may be attributed to the relative insensitivity of the anti-transition state to the variation of the $\beta$-aryl substituent.

All of these results are consistent with a slightly E1cb-like transition state for **1** and a more symmetrical transition state for **2**, respectively, as depicted in Figure 1. For both reactions, the structures of the transition states changes only slightly with the variation of the $\beta$-aryl substituent and the leaving group.

In conclusion, the nitrile-forming anti-eliminations from **2** proceed at a 36000 fold faster rate than that for **1** via more symmetrical transition states with a smaller degree of proton transfer, less negative charge development at the $\beta$-carbon, and a smaller extent of leaving group bond cleavage. The extent of proton transfer and negative charge density at the $\beta$-carbon decreases with a better leaving group, and the extent of the leaving group departure decreases with the electron-withdrawing ability of the $\beta$-aryl substituent. Noteworthy is the relative insensitivity of both transition states to the structural variations in the reactants.

## Experimental Section

**Materials.** (*E*)- and (*Z*)-Bezaldoximes were synthesized as reported previously.[1,3] All of the (*E*)-benzaldehyde *O*-benzoyloximes **1** were prepared in reasonable yields by slowly adding (*E*)-benzaldoximes (5.0 mmol) to the solution of substituted benzoyl chloride (5.5 mmol) in 7.0 mL of pyridine at room temperature. The solution was stirred for 1 h and poured into 70 mL of ice−water. The products were recrystallized from ethanol. The deuterated compounds **1aa**′−**d**′-$d_1$ and **1da**′-$d_1$ were prepared by using the benzaldehyde-$d_1$ and *p*-nitrobenzaldehyde-$d_1$ by the same procedure.[1,3−5] The spectral and analytical data of the compounds were consistent with the proposed structures. The yield (%), melting point (°C), IR (KBr, C=O, $cm^{-1}$), NMR (DMSO-$d_6$), and combustion analysis data for the new compounds are as follows.

**(*E*)-$C_6H_5CD$=NOC(O)$C_6H_5$ (1aa′-$d_1$)**: yield 59%; mp 96−97 °C; IR 1742; NMR $\delta$ 7.52−7.63 (m, 5H), 7.73 (t, 1H, $J$ = 7.2), 7.83 (d, 2H, $J$ = 7.7), 8.08 (d, 2H, $J$ = 7.3). Anal. Calcd for $C_{14}H_{10}DNO_2$: C, 74.32; H, 5.35; N, 6.19. Found: C, 74.41; H, 5.10; N, 6.23.

**(*E*)-$C_6H_5CH$=NOC(O)$C_6H_4$-*p*-OMe (1ab′)**: yield 48%; mp 95−97 °C; IR 1735; NMR $\delta$ 3.84 (s, 3H), 7.10 (d, 2H, $J$ = 8.9), 7.50−7.54 (m, 3H), 7.77−7.82 (m, 2H), 8.01 (d, 2H, $J$ = 8.9), 8.88 (s, 1H). Anal. Calcd for $C_{15}H_{13}NO_3$: C, 70.58; H, 5.13; N, 5.49. Found: C, 70.64; H, 5.13; N, 5.32.

**(*E*)-$C_6H_5CD$=NOC(O)$C_6H_4$-*p*-OMe (1ab′-$d_1$)**: yield 64%; mp 95−97 °C; IR 1733; NMR $\delta$ 3.88 (s, 3H), 7.13 (d, 2H, $J$ = 8.8), 7.56−7.60 (m, 3H), 7.82−7.87 (m, 2H), 8.04 (d, 2H, $J$ = 8.8). Anal. Calcd for $C_{15}H_{12}DNO_3$: C, 70.30; H, 5.51; N, 5.46. Found: C, 70.64; H, 5.16; N, 5.20.

**(*E*)-$C_6H_5CH$=NOC(O)$C_6H_4$-*m*-Br (1ac′):** yield 43%; mp 93−94 °C; IR 1739; NMR $\delta$ 7.56−7.60 (m, 4H), 7.78−7.82 (m, 2H), 7.94 (d, 1H, $J$ = 8.8), 8.05 (d, 1H, $J$ = 7.2), 8.20 (s, 1H), 8.98 (s, 1H). Anal. Calcd for $C_{14}H_{10}BrNO_2$: C, 55.29; H, 3.31; N, 4.61. Found: C, 55.33; H, 3.44; N, 4.60.

**(*E*)-$C_6H_5CD$=NOC(O)$C_6H_4$-*m*-Br (1ac′-$d_1$)**: yield 24%; mp 91−93 °C; IR 1742; NMR $\delta$ 7.55−7.61 (m, 4H), 7.81−7.83 (m, 2H), 7.95 (d, 1H, $J$ = 8.2), 8.07 (d, 1H, $J$ = 9.0), 8.21 (s, 1H). Anal. Calcd for $C_{14}H_9DBrNO_2$: C, 55.11; H, 3.63; N, 4.59. Found: C, 55.23; H, 3.38; N, 4.51.

**(*E*)-$C_6H_5CH$=NOC(O)$C_6H_4$-*p*-$NO_2$ (1ad′)**: yield 63%; mp 162−164 °C; IR 1744; NMR $\delta$ 7.52−7.59 (m, 3H), 7.79−7.83 (m, 2H), 8.28 (d, 2H, $J$ = 8.9), 8.40 (d, 2H, $J$ = 8.9), 8.97 (s, 1H). Anal. Calcd for $C_{14}H_{10}N_2O_4$: C, 62.22; H, 3.73; N, 10.37. Found: C, 62.15; H, 3.84; N, 10.32.

**(*E*)-$C_6H_5CD$=NOC(O)$C_6H_4$-*p*-$NO_2$ (1ad′-$d_1$)**: yield 34%; mp 163−164 °C; IR 1741; NMR $\delta$ 7.52−7.59 (m, 3H), 7.79−7.84 (m, 2H), 8.31 (d, 2H, $J$ = 8.7), 8.43 (d, 2H, $J$ = 8.7). Anal. Calcd for $C_{14}H_9DN_2O_4$: C, 62.00; H, 4.08; N, 10.33. Found: C, 62.07; H, 3.88; N, 10.31.

**(*E*)-*p*-$MeOC_6H_4CH$=NOC(O)$C_6H_4$-*m*-Br (1bc′)**: yield 38%; mp 110−112 °C; IR 1743; NMR $\delta$ 3.82 (s, 3H), 7.07 (d, 2H, $J$ = 8.9), 7.54 (t, 1H, $J$ = 8.0), 7.74 (d, 2H, $J$ = 8.9), 7.90 (d, 1H, $J$ = 8.2), 8.03 (d, 1H, $J$ = 8.2), 8.17 (s, 1H), 8.86 (s, 1H). Anal. Calcd for $C_{15}H_{12}BrNO_3$: C, 53.91; H, 3.62; N, 4.19. Found: C, 53.94; H, 3.59; N, 4.22.

**(*E*)-*m*-$BrC_6H_4CH$=NOC(O)$C_6H_5$ (1ca′)**: yield 99%; mp 117−119 °C; IR 1749; NMR $\delta$ 7.35 (t, 1H, $J$ = 7.9), 7.48−7.54 (m, 2H), 7.61−7.66 (m, 2H), 7.73 (d, 1H, $J$ = 7.7), 8.02 (s, 1H), 8.13 (d, 2H, $J$ = 7.0), 8.52 (s, 1H). Anal. Calcd for $C_{14}H_{10}BrNO_2$: C, 55.29; H, 3.31; N, 4.61. Found: C, 55.32; H, 3.31; N, 4.50.

**(*E*)-*m*-$BrC_6H_4CH$=NOC(O)$C_6H_4$-*p*-OMe (1cb′)**: yield 49%; mp 130−132 °C; IR 1737; NMR $\delta$ 3.81 (s, 3H), 7.06 (d, 2H, $J$ = 9.0), 7.44 (t, 1H, $J$ = 7.8), 7.70−7.78 (m, 2H), 7.92−7.98 (m, 3H), 8.83 (s, 1H). Anal. Calcd for $C_{15}H_{12}BrNO_3$: C, 53.91; H, 3.62; N, 4.19. Found: C, 53.97; H, 3.58; N, 4.08.

**(*E*)-*m*-$BrC_6H_4CH$=NOC(O)$C_6H_4$-*m*-Br (1cc′)**: yield 46%; mp 137−139 °C; IR 1745; NMR $\delta$ 7.42−7.61 (m, 2H), 7.75 (t, 2H, $J$ = 7.8), 7.89−7.97 (m, 2H), 8.02 (d, 1H, $J$ = 8.0), 8.17 (s, 1H), 8.95 (s, 1H). Anal. Calcd for $C_{14}H_9Br_2NO_2$: C, 43.90; H, 2.37; N, 3.66. Found: C, 43.75; H, 2.41; N, 3.62.

**(*E*)-*m*-$BrC_6H_4H$=NOC(O)$C_6H_4$-*p*-$NO_2$ (1cd′)**: yield 74%; mp 163−165 °C; IR 1755; NMR $\delta$ 7.44−7.56 (m, 1H), 7.75−7.84 (m, 2H), 8.00 (s, 1H), 8.27 (d, 2H, $J$ = 8.0), 8.40 (d, 2H, $J$ = 8.0), 8.96 (s, 1H). Anal. Calcd for $C_{14}H_9BrN_2O_4$: C, 48.16; H, 2.60; N, 8.02. Found: C, 48.26; H, 2.62; N, 7.95.

**(*E*)-*p*-$O_2NC_6H_4CD$=NOC(O)$C_6H_5$ (1da′-$d_1$)**: yield 44%; mp 177−179 °C; IR 1742; NMR $\delta$ 7.44 (t, 2H, $J$ = 8.1), 7.55−7.60 (m, 1H), 7.94 (d, 2H, $J$ = 8.9), 8.07 (d, 2H, $J$ = 7.2), 8.26 (d, 2H, $J$ = 8.9). Anal. Calcd for $C_{14}H_9DN_2O_4$: C, 62.00; H, 4.08; N, 10.33. Found: C, 62.00; H, 4.11; N, 10.58.

**(*E*)-*p*-$O_2NC_6H_4CH$=NOC(O)$C_6H_4$-*p*-OMe (1db′)**: yield 61%; mp 180-183 °C; IR 1738; NMR $\delta$ 3.85 (s, 3H), 7.11 (d, 2H, $J$ = 7.8), 8.06 (d, 2H, $J$ = 9.0), 8.02 (d, 2H, $J$ =7.8), 8.35 (d, 2H, $J$

= 9.0), 9.05 (s, 1H). Anal. Calcd for $C_{15}H_{12}N_2O_5$: C, 60.00; H, 4.03; N, 9.33. Found: C, 60.00; H, 4.11; N, 9.24.

**(*E*)-*p*-$O_2NC_6H_4CH$=NOC(O)$C_6H_4$-*m*-Br (1dc′)**: yield 44%; mp 183−185 °C; IR 1764; NMR $\delta$ 7.56 (t, 1H, $J$ = 8.0), 7.92-8.19 (m, 4H), 8.19 (s, 1H), 8.35 (d, 2H, $J$ = 7.0), 9.13 (s, 1H). Anal. Calcd for $C_{14}H_9BrN_2O_4$: C, 48.16; H, 2.60; N, 8.02. Found: C, 48.30; H, 2.64; N, 7.94.

**(*E*)-*p*-$O_2NC_6H_4H$=NOC(O)$C_6H_4$-*p*-$NO_2$ (1dd′)**: yield 58%; mp 191−193 °C; IR 1742; NMR $\delta$ 8.09 (d, 2H, $J$ = 9.2), 8.30 (d, 2H, $J$ = 9.0), 8.38 (d, 2H, $J$ = 9.2), 8.42 (d, 2H, $J$ = 9.0), 9.16 (s, 1H). Anal. Calcd for $C_{14}H_9N_3O_6$: C, 53.34; H, 2.88; N, 13.33. Found: C, 53.50; H, 2.90; N, 13.22.

(*Z*)-Benzaldehyde *O*-benzoyloxime derivatives were synthesized by the following procedures. The deuterated compounds **2ab′**−**d′**-$d_1$ and **2da′**-$d_1$ were prepared by using benzaldehyde-$d_1$ and *p*-nitrobenzaldehyde-$d_1$ by the same procedure.[1,3−5] However, compounds **2ba′**, **2bb′**, and **2dd′**were too unstable to isolate from the reaction mixture.

**(i) Procedure A.** (*Z*)-Benzaldoximes (5.0 mmol) were slowly added to a solution containing substituted benzoyl chloride (1.7 mmol) in 5.0 mL of pyridine at −35 to −40 °C. The solution was stirred for 1−30 min. To this solution were added 20 mL of −10 °C methanol and 50 mL of ice−water. The solid products were dissolved in the minimum amount of $CH_2Cl_2$ and recrystallized by adding 5 mL of MeOH−15 mL of $H_2O$ at −10 to −15 °C. Compounds **2aa′**, **2ba′**, **2ca′**, **2da′**, **2bc′**, **2bd′**, and **2aa′**-$d_1$ were obtained in reasonable yields by this procedure. Compounds **2da′**-$d_1$, **2cb′**, and **2db′** were synthesized by the same procedure except that **2d**,**a′**-$d_1$ was recrystallyzed three times by adding 5 mL of $H_2O$ to the methanolic solution of the product, and **2cb′** and **2db′** were crystallized from 10 mL of benzene−30 mL of hexane at −10 to −15 °C, respectively.

**(ii) Procedure B.** (*Z*)-Benzaldoximes (0.66 mmol) and pyridine (0.05 g, 0.06 mmol) were slowly added to a solution containing substituted benzoyl chloride (0.90 mmol) in 5.0 mL of THF at −78 °C. The solution was stirred for 5−10 min. To this solution was added 30 mL of −10 °C methanol and 50 mL of ice−water. The solid product was filtered while it was cold and recrystallized from 10 mL of MeOH/$H_2O$ = 3/1 at −10 to −15 °C. Compounds **2ac′**, **2cc′**, **2dc′**, **2ad′**, **2cd′**, **2ac′**-$d_1$, and **2ad′**-$d_1$ were prepared by this procedure. **2dd′** was prepared by the same procedure except that the product was recrystallyzed from MeOH at −15 °C.

The yield (%), melting point (°C), IR (KBr, C=O, $cm^{-1}$), NMR ($CDCl_3$), and combustion analysis data for the new compounds are as follows.

**(*Z*)-$C_6H_5CH$=NOC(O)$C_6H_5$ (2aa′)**: yield 36%; mp 57−58 °C; IR 1742; NMR $\delta$ 7.47−7.68 (m, 7H), 7.87−7.92 (m, 2H), 8.08−8.18 (m, 2H). Anal. Calcd for $C_{14}H_{11}NO_2$: C, 74.65; H, 4.92; N, 6.22. Found: C, 74.68; H, 4.95; N, 6.16.

**(*Z*)-$C_6H_5CD$=NOC(O)$C_6H_5$ (2aa′-$d_1$)**: yield 47%; mp 55−57 °C; IR 1741; NMR $\delta$ 7.47−7.64 (m, 6H), 7.88−7.93 (m, 2H), 8.09−8.13 (m, 2H). Anal. Calcd for $C_{14}H_{10}DNO_2$: C, 74.32; H, 5.35; N, 6.19. Found: C, 74.43; H, 5.04; N, 5.83.

**(*Z*)-$C_6H_5CH$=NOC(O)$C_6H_4$-*m*-Br (2ac′)**: yield 35%; mp 71−73 °C; IR 1767; NMR $\delta$ 7.33 (dd, 1H, $J$ = 7.8, 8.1), 7.47−7.49 (m, 3H), 7.70 (d, 1H, $J$ = 7.8), 7.79−7.82 (m, 2H), 7.88 (s, 1H), 7.96 (d, 1H, $J$ = 8.1), 8.18 (s, 1H). Anal. Calcd for $C_{14}H_{10}BrNO_2$: C, 55.29; H, 3.31; N, 4.61. Found: C, 55.46; H, 3.45; N, 4.18.

**(*Z*)-$C_6H_5CD$=NOC(O)$C_6H_4$-*m*-Br (2ac′-$d_1$)**: yield 16%; mp 72−74 °C; IR 1766; NMR $\delta$ 7.33 (dd, 1H, $J$ = 7.8, 8.1), 7.43−7.52 (m, 3H), 7.70 (d, 1H, $J$ = 7.8), 7.78−7.85 (m, 2H), 7.96 (d, 1H, $J$ = 8.1), 8.18 (s, 1H). Anal. Calcd for $C_{14}H_9DBrNO_2$: C, 55.10; H, 3.63; N, 4.59. Found: C, 55.21; H, 3.32; N, 4.34.

**(*Z*)-$C_6H_5CH$=NOC(O)$C_6H_4$-*p*-$NO_2$ (2ad′)**: yield 45%; mp 119−120 °C (dec); IR 1752; NMR $\delta$ 7.50−7.60 (m, 3H), 7.82−7.86 (m, 2H), 7.98 (s, 1H), 8.26 (d, 2H, $J$ = 8.7), 8.37 (d, 2H, $J$ = 8.7). Anal. Calcd for $C_{14}H_{10}N_2O_4$: C, 62.22; H, 3.73; N, 10.37. Found: C, 62.23; H, 3.74; N, 10.26.

**(*Z*)-$C_6H_5CD$=NOC(O)$C_6H_4$-*p*-$NO_2$ (2ad′-$d_1$)**: yield 51%; mp 121−123 °C (dec); IR 1752; NMR $\delta$ 7.50−7.58 (m, 3H), 7.82−7.88 (m, 2H), 8.26 (d, 2H, $J$ = 9.0), 8.37 (d, 2H, $J$ = 9.0). Anal. Calcd for $C_{14}H_9DN_2O_4$: C, 62.00; H, 4.08; N, 10.33. Found: C, 62.07 ; H, 3.83; N, 10.28.

**(*Z*)-*p*-$MeOC_6H_4CH$=NOC(O)$C_6H_5$ (2ba′)**: yield 43%; mp 56−58 °C; IR 1741; NMR $\delta$ 3.87 (s, 3H), 7.00 (d, 2H, $J$ = 8.8), 7.46−7.53 (m, 2H), 7.61 (t, 1H, $J$ = 7.4), 7.80 (s, 1H), 7.90 (d, 2H, $J$ = 8.8), 8.12 (d, 2H, $J$ = 7.8). Anal. Calcd for $C_{15}H_{13}NO_3$: C, 70.58; H, 5.13; N, 5.49. Found: C, 70.56; H, 5.14; N, 5.57.

**(*Z*)-*p*-$MeOC_6H_4CH$=NOC(O)$C_6H_4$-*m*-Br (2bc′)**: yield 39%; mp 84−85 °C; IR 1759; NMR $\delta$ 3.89 (s, 3H), 7.02 (d, 2H, $J$ = 8.8), 7.40 (t, 1H, $J$ = 7.8), 7.75 (d, 1H, $J$ =7.8), 7.81 (s, 1H), 7.83 (d, 2H, $J$ = 8.8), 8.04 (d, 1H, $J$ = 7.8), 8.26 (s, 1H). Anal. Calcd for $C_{15}H_{12}BrNO_3$: C, 53.91; H, 3.62; N, 4.19. Found: C, 53.94; H, 3.59; N, 3.92.

**(*Z*)-*p*-$MeOC_6H_4CH$=NOC(O)$C_6H_4$-*p*-$NO_2$ (2bd′)**: yield 25%; mp 118-119 °C (dec); IR 1758; NMR $\delta$ 3.90 (s, 3H), 7.02 (d, 2H, $J$ = 9.0), 7.85 (d, 2H, $J$ = 9.0), 7.85 (s, 1H), 8.28 (d, 2H, J = 8.8), 8.38 (d, 2H, $J$ = 8.8). Anal. Calcd for $C_{15}H_{12}N_2O_5$: C, 60.00; H, 4.03; N, 9.33. Found: C, 60.04; H, 3.85; N, 9.25.

**(*Z*)-*m*-$BrC_6H_4CH$=NOC(O)$C_6H_5$ (2ca′)**: yield 30%; mp 78−80°C; IR 1749; NMR $\delta$ 7.41−7.75 (m, 6H), 7.88 (s, 1H), 8.07−8.16 (m, 3H). Anal. Calcd for $C_{14}H_{10}BrNO_2$: C, 55.29; H, 3.31; N, 4.61. Found: C, 55.29; H, 3.36; N, 4.42.

**(*Z*)-*m*-$BrC_6H_4CH$=NOC(O)$C_6H_4$-*p*-OMe (2cb′)**: yield 42%; mp 86−88 °C; IR 1746; NMR $\delta$ 3.90 (s, 3H), 7.00 (d, 2H, $J$ = 8.7), 7.41 (t, 1H, $J$ = 7.8), 7.66 (d, 1H, $J$ = 7.8), 7.76 (d, 1H, $J$ = 7.8), 7.86 (s, 1H), 8.06 (d, 2H, $J$ = 8.7), 8.15 (s, 1H). Anal. Calcd for $C_{15}H_{12}BrNO_3$: C, 53.91; H, 3.62; N, 4.19. Found: C, 53.87; H, 3.63; N, 4.14.

**(*Z*)-*m*-$BrC_6H_4CH$=NOC(O)$C_6H_4$-*m*-Br (2cc′)**: yield 52.6%; mp 86.5−88.5 °C; IR 1758; NMR $\delta$ 7.31−7.38 (m, 2H), 7.61−7.71 (m, 3H), 7.83 (s, 1H), 7.96 (d, 1H, $J$ = 7.9), 8.08 (s, 1H), 8.16 (s, 1H). Anal. Calcd for $C_{14}H_9Br_2NO_2$: C, 43.9; H, 2.37; N, 3.66. Found: C, 43.94; H, 2.28; N, 3.45.

**(*Z*)-*m*-$BrC_6H_4H$=NOC(O)$C_6H_4$-*p*-$NO_2$ (2cd′)**: yield 48%; mp 125−127 °C (dec); IR 1758; NMR $\delta$ 7.43 (t, 1H, $J$ = 7.6), 7.71 (d, 2H, $J$ = 7.6), 7.94 (s, 1H), 8.11 (s, 1H), 8.26 (d, 2H, $J$ = 8.4), 8.41 (d, 2H, $J$ = 8.4). Anal. Calcd for $C_{14}H_9BrN_2O_4$: C, 48.16; H, 2.60; N, 8.02. Found: C, 48.33; H, 2.75; N, 7.80.

**(*Z*)-*p*-$O_2NC_6H_4H$=NOC(O)$C_6H_5$ (2da′)**: yield 55%; mp 96−98 °C; IR 1758; NMR $\delta$ 7.52 (dd, 2H, $J$ = 7.6, 8.7), 7.65 (t, 1H, $J$ = 7.6), 8.05 (d, 4H, $J$ = 8.7), 8.07 (s, 1H), 8.39 (d, 2H, $J$ = 8.8). Anal. Calcd for $C_{14}H_{10}N_2O_4$: C, 62.22; H, 3.73; N, 10.37. Found: C, 62.24; H, 3.77; N, 10.13.

**(*Z*)-*p*-$O_2NC_6H_4CD$=NOC(O)$C_6H_5$ (2da′-$d_1$)**: yield 11%; mp 102−104 °C; IR 1760; NMR $\delta$ 7.51 (dd, 2H, $J$ = 7.5, 8.7), 7.66 (t, 1H, $J$ = 7.5), 8.05 (d, 4H, $J$ = 8.7), 8.39 (d, 2H, $J$ = 8.7). Anal. Calcd for $C_{14}H_9DN_2O_4$: C, 62.00; H, 4.08; N, 10.33. Found: C, 62.30; H, 4.05; N, 10.00.

**(*Z*)-*p*-$O_2NC_6H_4CH$=NOC(O)$C_6H_4$-*p*-OMe (2db′)**: yield 40%; mp 115−117 °C; IR 1762; NMR $\delta$ 3.90 (s, 3H), 7.00 (d, 2H, $J$ = 9.0), 8.01 (d , 2H, $J$ = 9.0), 8.04 (s, 1H), 8.05 (d, 2H, $J$ = 8.8), 8.39 (d, 2H, $J$ = 8.8). Anal. Calcd for $C_{15}H_{12}N_2O_5$: C, 60.00; H, 4.03; N, 9.33. Found: C, 60.00; H, 4.03; N, 9.16.

**(*Z*)-*p*-$O_2NC_6H_4CH$=NOC(O)$C_6H_4$-*m*-Br (2dc′)**: yield 48%; mp 104−106 °C; IR 1756; NMR $\delta$ 7.34 (dd, 1H, $J$ = 7.5, 8.1), 7.72 (d, 1H, $J$ = 8.1), 7.89 (d, 1H, $J$ = 7.5), 7.82 (d, 2H, $J$ = 8.5), 8.02 (s, 1H), 8.12 (s, 1H), 8.34 (d, 2H, $J$ = 8.5). Anal. Calcd for $C_{14}H_9BrN_2O_4$: C, 48.16; H, 2.60; N, 8.02. Found: C, 48.35; H, 2.82; N, 7.83.

1,8-Diazabicyclo[5.4.0]undec-7-ene (DBU) was redistilled in vacuo prior to use, and acetonitrile has been purified as described before.[1] Solutions of DBU in MeCN were prepared by dissolving DBU in MeCN.

**Kinetic Studies.** Reactions of (*E*)-benzaldehyde *O*-benzoyloximes with DBU in MeCN were followed by monitoring the decrease in the absorption of the reactants at 260−292 nm with a UV-vis spectrophotometer or a stopped-flow spectrophotometer as described before.[1] On the other hand, reactions of **1aa′**−**c′**, **1ba′**−**c′**, and their deuterated analogs with DBU were too slow to measure the infinity absorption values accurately. Therefore, a Guggenheim method was employed.

**Product Studies.** The yields of PhC≡N from the reactions of **1aa′** and **2aa′** with DBU were determined by GC as

described previously.[1,3] The yields were 99 and 93% for **1aa′** and **2aa′**, respectively.

**Control Experiments.** The stability of **1aa′**, **2aa′**, and their solutions were determined by measuring the melting point and periodical scanning of the solutions with the UV spectrophotometer.[1,3] No change in melting point or UV spectrum was detected for **1aa′** during 6 months in the refrigerator. On the other hand, **2aa′** and solutions **1aa′** and **2aa′** in MeCN were stable for 1 week when stored in the refrigerator.

**Acknowledgment.** This research was supported by Korea Research Foundation (Project No. 97-001-D00237).

**Supporting Information Available:** Hammett plots for eliminations from (*E*)-$XC_6H_4CL{=}NOC(O)C_6H_4Y$ and (*Z*)-$XC_6H_4CL{=}NOC(O)C_6H_4Y$ promoted by DBU in MeCN at 25.0 °C, plots of log $k_2$ vs p$K_{1g}$ values for eliminations from (*E*)-$XC_6H_4CL{=}NOC(O)C_6H_4Y$ and (*Z*)-$XC_6H_4CL{=}NOC(O)C_6H_4Y$ promoted by DBU in MeCN at 25.0 °C, and structures of (*E*)- and (*Z*)-benzaldehyde *O*-benzoyloximes calculated by the Gaussian 94, Revision A.1 with 6-311G basis set (5 pages). This material is contained in libraries on microfiche, immediately follows this article in the microfilm version of the journal, and can be ordered from the ACS; see any current head masthead page for ordering information.

JO980264S